Published in final edited form as:
Cancer Lett. 2011 January 28; 300(2): 154–161. doi:10.1016/j.canlet.2010.09.017.

ABCA2 transporter deficiency reduces incidence of TRAMP prostate tumor metastasis and cellular chemotactic migration

Jody T. Mack[a], **Kristi L. Helke**[b], **Gabrielle Normand**[a], **CoDanielle Green**[c], **Danyelle M. Townsend**[c], and **Kenneth D. Tew**[a,*]

[a]Department of Cell and Molecular Pharmacology and Experimental Therapeutics, Medical University of South Carolina, Charleston, South Carolina 29425

[b]Department of Comparative Medicine/Division of Laboratory Animal Resources, Medical University of South Carolina, Charleston, South Carolina 29425

[c]Department of Pharmaceutical and Biomedical Sciences, Medical University of South Carolina, Charleston, South Carolina 29425

Abstract

In order to study the effects of ATP-binding cassette transporter 2 (ABCA2) deficiency on the progression of prostate cancer, congenic Abca2 knockout (KO) mice were crossed to the transgenic adenocarcinoma of the mouse prostate (TRAMP) model. ABCA2 expression was elevated in wild-type/TRAMP (WT/Tg) dorsal prostate, a region comprising the most aggressive tumors in this model, compared to non-transgenic WT mice. Primary prostate tumor progression was similar in KO/Tg and WT/Tg mice with respect to pathological score, prostate tumor growth, as calculated using MRI volumetry, and proliferative index, as determined by PCNA immunostaining. Vimentin, a marker of the epithelial-mesenchymal transition, was expressed at similar levels in prostate, but elevated in histologically normal seminal vesicles (SV) in KO/Tg mice ($P < 0.02$), concomitant with an increased SV volume ($P < 0.01$). These changes in the SV did not exacerbate the metastatic phenotype of this disease model; rather, KO/Tg mice aged 20-25 weeks had no detectable metastases while 38% of WT/Tg developed metastases to lung and/or lymph nodes. The absence of a metastatic phenotype in KO/Tg mice was reprised in stable ABCA2 knockdown (KD) cells where chemotactic, but not random, migration was impaired ($P = 0.0004$). Expression levels of sphingolipid biosynthetic enzymes were examined due to the established link of the transporter with sphingolipid homeostasis. Galactosylceramide synthase (GalCerS) mRNA levels were over 8-fold higher in KD cells ($P = 0.001$), while lactosylceramide synthase (LacCerS) and CTP:choline cytidylyltransferase (CCT) were significantly reduced ($P < 0.0001$ and 0.03, respectively). Overall, we demonstrate that ABCA2 deficiency inhibits prostate tumor metastasis *in vivo* and decreases chemotactic potential of cells, conceivably due to altered sphingolipid metabolism.

*Corresponding author. Department of Cell and Molecular Pharmacology, Medical University of South Carolina, 96 Jonathan Lucas Street, CSB/313G, P.O. Box 250505, Charleston, SC 29425. Fax: +1 843 792 9588. tewk@musc.edu..

Conflicts of Interest Statement
None Declared

Keywords

TRAMP; ABC transporter; prostate; chemotaxis; metastasis

1. Introduction

The ATP-binding cassette transporter 2 (ABCA2) is an endolysosomal protein associated with lipid transport and drug resistance [1]. *In vivo*, the transporter is primarily expressed in the central and peripheral nervous systems, prostate, ovary and macrophages [2;3;4;5]. The transporter is purported to function in sphingolipid transport for the development/ homeostasis of cellular membranes [1], especially that of myelin sheath in the central nervous system [6;7]. Prostate and ovarian cancer cell lines, [2], and a growing number of human neurological and hematological cancers, have elevated expression of ABCA2 [1]. Prostate and ovarian cancer cell lines resistant to estramustine (EM), an anti-microtubule agent used in prostate cancer chemotherapy, have augmented ABCA2 levels compared to parental cell lines [3;8;9]. Studies have linked ABCA2 expression with endolysosomal compartmentalization of lipophilic substrates, such as estramustine, and resistance to such agents [2;3;10]. High ABCA2 expression was also shown in a side population (SP) of stem-like cells in lung cancer cell lines [11]. These SP cells demonstrated a higher capacity for tumor initiation and invasion in tumor xenografts. ABCA5, a related lysosomal ABC transporter, was recently shown as a sensitive urine diagnostic marker for high-grade prostatic intraepithelial neoplasia [12].

Our laboratory characterized the physiological effects of ABCA2 deficiency by generating an ABCA2 knockout (KO) mouse [6]. This together with an independent report by Sakai and colleagues [7] demonstrated that ABCA2 deficiency produces a smaller body size, a shaking phenotype concomitant with changes in myelin ultrastructure [6] or sphingolipid composition [7] of neuronal tissues. Higher levels of gangliosides and lower levels of sphingomyelin (SM) in whole brain and myelin fractions [7] implied a role for this transporter in sphingolipid metabolism. Overall, the mouse phenotype implicated a role for ABCA2 in the development/maintenance of myelin membrane and sphingolipid homeostasis.

Cancer cells, and specifically, prostate cancer cells, rely on elevated SM levels to maintain a highly metastatic phenotype [13]. In turn, sphingolipid signaling influences tumor cell growth, survival and apoptosis [14]. Given the elevated expression of ABCA2 in human prostate cancer cells and drug-resistant sub-lines and the impact of ABCA2 deficiency on sphingolipid metabolism, we sought to determine what role ABCA2 may play in prostate tumor development and progression. To accomplish this objective, we utilized our Abca2 knockout line in the context of the TRAMP (transgenic adenocarcinoma of the mouse prostate) mouse, an established metastatic prostate tumor model [15;16]. Mice hemizygous for the transgene express the SV40/ T/t antigen downstream of the prostate-specific rat probasin promoter and mimic the spectrum of human prostate tumorigenesis. Mice develop prostatic intraepithelial neoplasia (PIN) by 12 weeks of age and well-differentiated adenocarcinoma by 24 weeks with metastatic lesions to the liver, lung and/or pelvic lymph nodes in most animals by 30 weeks. Seminal vesicle tumors of stromal origin also appear with a phyllodes tumor appearance [17], and with the exception of one report [18], do not typically progress to malignant tumors.

In order to determine the importance of ABCA2 in cellular chemotaxis and metastasis, we employed a semi-differentiated Schwann cell model (D6P2T) that was previously characterized for the study of galactolipid synthesis, transport and sorting [19]. These cells

have also demonstrated a metastatic phenotype using cell motility assays [20]. In our present study, both the *in vivo* and *in vitro* results support the concept that ABCA2 deficiency may delay the presentation of metastatic tumors in TRAMP mice and inhibit cellular chemotactic migration.

2. Materials and methods

2.1. Animals

TRAMP (WT/Tg) mice on a C57BL/6 background were purchased from Jackson Laboratories (C57BL/6-Tg (TRAMP)8247Ng/J) and crossed to the Abca2 knockout (KO; [6]) line on a congenic C57BL/6 background. Heterozygous progeny (ABCA2+/−/Tg) were crossed together to generate Abca2+/+/Tg (WT/Tg) and Abca2−/−/Tg (KO/Tg) littermates. Animals were housed in microisolation cages and maintained in a climate-controlled facility (68°F–72°F) with a 12h light/dark cycle and were supplied with tap water and a specific rodent diet (5K67, Lab Diet, PMI Nutrition International) *ad libitum* from weaning. Animal experiments were conducted in accordance with the MUSC Institutional Animal Care and Use Committee.

2.2. Magnetic resonance imaging (MRI)

Three-dimensional MRI was acquired with a rapid acquisition with relaxation enhancement (RARE) sequence on a 7 Tesla Bruker system **(**Bruker AXS Inc., Madison, WI). Scans were conducted with no contrasting agents as previously described [21] in the Preclinical Imaging in Translational Research Core facility under the direction of Dr. Mehmet Bilgen. Mice were anesthetized using isofluorane gas (1-4% for induction in a chamber, followed by 1-4% plus 30% oxygen for maintenance). The anesthetized animals were placed on a Plexiglas sled, connected to a respiratory monitoring system, and positioned in the scanner for imaging. Sixty adjacent coronal MRI images (0.5mm slices) of the genitourinary apparatus were acquired for each animal.

2.3. Volumetric analysis of MRI acquisitions

Images were analyzed using NIH Image J software. Images were opened as Raw 2D sequence files (256 × 256 pixels) and area of the seminal vesicles and prostate were measured for each of 60, 0.5mm slices in triplicate. Slice volume was calculated by multiplying average pixel area by a calibrator (2.4336×10^{-4} cm^2/pixel), followed by the height of the slice (0.05 cm). The volume of the SV and prostate were calculated by the sum of the slice volumes.

2.4. Immunohistochemistry (IHC)

Tissues were fixed in plastic tissue cassettes and fixed overnight in 4% paraformaldehyde/PBS pH 7.4 and processed at the Histology Core facility (MUSC Dept. of Pathology & Laboratory Medicine). Paraffin sections were dewaxed and rehydrated using SafeClear II (Fisher Scientific) followed by an ethanol series. After washing twice in dH_2O, antigen retrieval was carried out using a steamer bath in 10mM sodium citrate pH 6.0 for 30 min. Endogenous peroxidase activity was blocked by a 10 min incubation in 3%H_2O_2/methanol at room temperature. Sections were then blocked in 10% goat or horse serum (for rabbit or mouse primary antibodies, respectively) containing 0.1% Triton X-100 and 1% bovine serum albumin in phosphate buffered saline (PBS) pH 7.4. Sections were incubated in primary antibody diluted in blocking agent overnight at 4° C. at the following dilutions: ABCA2 [6], 1:500; 8-OHdG (Abcam), 1:100; 4HNE (Calbiochem), 1:100; vimentin (Santa Cruz), 1:150; desmin (Abcam), 1:200; PCNA (Abcam), 1:400. Slides were developed using the rabbit or mouse UniTect™ ABC kit (Calbiochem) per the manufacturer's instructions,

counterstained in 10% hematoxylin/dH_2O (Fisher Scientific) and analyzed by light microscopy.

2.5. *Pathological and IHC scoring*

GU tract tissues were fixed and processed as stated above, stained with hematoxylin and eosin and pathologically scored as described in detail by Suttie and colleagues [16].

Sections subject to IHC were examined under light microscopy with 100× to 400× magnification. The sections were scored within a range of 0 to 300 by multiplying the staining intensity (no staining: 0; weak: 1+; moderate: 2+; strong: 3+) by the percentage of immunoreactive cells (0-100) for at least 20 high-powered fields. Similar immunoscoring systems have been used to evaluate clinical biopsies [22].

2.6.*Cell lines*

D6P2T cells stability transfected with the pKoen plasmid targeting knockdown of rat ABCA2 (KD) or a control shRNA (Ctr) were obtained from Dr. Hein Sprong (Department of Membrane Enzymology, Bijvoet Center and Institute of Biomembranes, Utrecht University). RT-PCR screening of ABCA2 knockdown was conducted using Superscript II reverse transcriptase (Invitrogen) and PCR with primers for ABCA2 and GAPDH loading control (Table 1) using a 2× Taq polymerase master mix (Eppendorf). Stable cell lines were maintained in Dulbecco's minimal essential media (DMEM; Invitrogen, Carlsbad, CA) 10% fetal calf serum (Mediatech Inc., Manassas, VA), 2 mM L-glutamine, 0.1 mM non-essential amino acids and 100 units/ml penicillin-streptomycin and 1 mg/ml G418 (Invitrogen).

2.7. *Immunblotting and quantitative real-time PCR*

Knockdown of ABCA2 by RT-PCR was confirmed and quantified using standard western blotting techniques with an anti-ABCA2 rabbit polyclonal antibody as described by Mack *et al.* [5]. Primer design, reverse transcription and real-time PCR were conducted as previously described [5]. SYBR-green detection of mRNAs listed in Table 1 was achieved with GAPDH as loading control (iCycler, BioRad, Hercules, CA).

2.8. *Cell migration and chemotaxis*

For each independent cell migration experiment, D6P2T Ctr and KD cells in log-phase growth were plated in 6 cm dishes, in triplicate, in complete media (10% FBS/DMEM) overnight to achieve a confluent monolayer. Cells were briefly washed in sterile PBS before and after scratch "wounds" to the monolayer were made using sterile 200 μl pipette tips. Cells were then covered with either complete media or serum-free media (SFM) and allowed to incubate at 37°C/5% CO_2 for 24 h. Several low-power images were captured using light microscopy (Nikon Instruments, Inc., Melville, NY) for specific areas marked on the outside of culture dishes at several time intervals up to 24 h. Gap width was measured in triplicate, using Image J software (National Institutes of Health, Bethesda, MD), and averaged for each image. For chemotaxis assays, 1.8×10^4 log-phase cells were plated in the top of a fibronectin-coated 8 μm pore-size transwell chamber (BD Biosciences) in a 24-well plate (Nunc) in either SFM or 10% FBS (complete media) in the top chamber and complete media in the bottom chamber during 18h incubation. Cells in the top chamber were removed with a cotton swab and cells that migrated to the bottom chamber were washed in PBS, and fixed for 15′ in 4% paraformaldehyde/PBS pH 7.4. Cells were stained using 0.1% crystal violet/ ddH_2O, counted by light microscopy. The index of chemotactic migration was defined as the number of cells in the bottom chamber (minus the background of random migration, *i.e.*, FBS in both chambers) as a percentage of total cells plated.

3. Results

3.1. ABCA2 is elevated in TRAMP prostate tumors compared to WT

Protein expression of ABCA2 was elevated in the dorsal prostate of WT/Tg mice (Fig. 1A), relative to WT littermates at 20 weeks of age (Fig. 1B). Dorsal prostatic tumors are generally found to be the most aggressive tumors [16]. The average ABCA2 immunoscore for WT dorsal prostate was significantly lower than for WT/Tg and Abca2$^{+/-}$/Tg (HET/Tg), but not for the KO or KO/Tg controls (Fig. 1C). ABCA2 immunostaining of KO and KO/Tg dorsal prostates established background, non-specific staining. Higher expression in the neoplastic epithelia of WT/Tg and HET/Tg were observed (as in Fig. 1A), contributing to higher immunoscores. This increased expression in WT/Tg tissue is supportive of a role for ABCA2 in the primary tumor of this disease model. Comparison of seminal vesicle tissue, both normal and tumor bearing, in WT versus WT/Tg or WT/Tg alone, showed absent or very low staining with the ABCA2 antibody, indicating low levels of the transporter in this tissue. Liver, a tissue with similar ABCA2 expression as prostate, was used as a control to assess any global changes in the context of the Tg model. No significant changes were observed among liver sections subjected to IHC between WT/Tg and WT mice (data not shown).

3.2. Similar primary tumor burden in WT/Tg and KO/Tg mice

The volume of the genitourinary tract is an index of tumor burden in the TRAMP model. Increased volume of prostatic tissue, as observed using magnetic resonance imaging (MRI), is consistent with an increased tumor burden and increased progression for the primary tumors in this model [21]. Volumetry was accomplished using magnetic resonance imaging at 20 weeks of age, and in the same animals at 25 weeks (Fig. 2A; $n = 5$ per genotype). The average prostate tissue volume was similar between WT/Tg and KO/Tg mice at both time points (Fig. 2A). This is consistent with the pathological analyses that reveal no significant change in primary tumor progression in the absence of ABCA2 expression ($P = 0.67$ and 0.47 for 20 and 25w, respectively; Table 2). Additionally, primary tumors of the dorsal prostate, the site of the most aggressive tumors in the TRAMP model [16], have similar proliferative indices in both WT/Tg and KO/Tg mice, as determined by proliferative cell nuclear antigen (PCNA) IHC (Fig. 2B). Similarly, the growth rates of prostate and SV (presented as change in mm^3 per g body weight) were not impacted by the Abca2 genotype (0.01 ± 0.02 vs. 0.02 ± 0.01 for prostate and 0.10 ± 0.03 vs. 0.11 ± 0.17 for SV in WT/Tg and KO/Tg, respectively; $P = 0.57$ and 0.95).

Vimentin, a marker of the epithelial-mesenchymal transition in metastatic tumor cells, was similarly expressed in the endothelium of WT/Tg and KO/Tg primary prostate lesions and surrounding normal tissue (data not shown; immunoscores determined at 20 and 25w, $P > 0.3$ for both).

Due to a previous study linking ABCA2 with oxidative stress response [23], we examined markers for oxidative stress damage to lipids (4-hydroxynonenal modified proteins; 4HNE) and DNA (8-hydroxydeoxyguanosine; 8-OHdG) in prostate and SV tissues at 20 and 25 weeks. No marked changes were present for 4HNE or 8-OHdG in the KO/Tg tissues compared to WT/Tg (data not shown; $P > 0.05$ for both).

3.3. Vimentin expression of histologically normal SV tissue and volume of SV are increased in KO/Tg at 20 weeks

At 20 weeks of age, KO/Tg mice had significantly larger seminal vesicles (SV) compared to aged-matched WT/Tg as determined by MRI volumetry (Fig. 3A-C). We sought to examine mesenchymal protein expression to characterize the lineage of stromal tumors present in SV

[17]. While no significant changes in vimentin or desmin expression were detected in stromal tumors of the SV ($P > 0.1$), there was an increase in vimentin expression in the normal SV tissue (lamina propria) of KO/Tg mice (Fig. 3E-G).

3.4. Metastatic lesions absent in ABCA2 KO/Tg mice

Although the progression of primary prostate tumors is similar in terms of prostate volume, pathology and proliferative index, KO/Tg mice (0%) lack the characteristic metastasis to lung and pelvic lymph nodes that their WT/Tg (38%) littermates show at 20 and 25 weeks of age (Table 2). Overall, more than half of the WT/Tg mice were found with either metastases or hyperplasia of the lung and/or lymph nodes, while no metastases or hyperplasia were observed in KO/Tg mice. In addition, large (>7g) poorly-differentiated tumor masses were observed at necropsy in a third of 20 to 30 week-old WT/Tg mice, while none were found in age-matched KO/Tg animals (Table 3).

3.5. ABCA2 knockdown inhibits chemotaxis in D6P2T cells

The shRNA-based knockdown (KD) of ABCA2 in stable D6P2T clones was confirmed by RT- and quantitative PCR and by immunoblot analysis compared to cells expressing a control shRNA construct (Ctr) (Fig. 4A,B). A significant reduction in ABCA2 transcript was shown using RT-PCR (75-80%) as well as quantitative real-time PCR (80%; $P = 0.0006$). This translated into a 75% decrease in ABCA2 protein signal observed by immunoblot. We utilized this cell model of ABCA2 deficiency due to the elevated basal expression of the transporter in the Ctr cell line. KD and Ctr cells had essentially equivalent migration rates during a wound-healing assay in both serum-free and 10%-FBS containing media (Fig. 4C). These cells were subjected to a transwell migration assay along a serum gradient. KD cells exhibit a significant decrease in the propensity to undergo chemotaxis from serum-free-to 10% serum-containing media (Fig, 4D; $*P = 0.0004$). The increased chemotatic activity of Ctr cells is not a result of increased migration, as observed when cells are plated in a transwell chamber with 10% serum in both chambers (data not shown), as supported by the wound-healing data. These results suggest that ABCA2 functions in the process of chemotactic, but not random, migration.

3.6. Changes in expression of sphingolipid biosynthetic enzymes

Transcript levels of glucosylceramide synthase (GlcCerS), galactosylceramide synthase (GalCerS), lactosylceramide synthase (LacCerS), CTP:choline cytidylyltransferase (CCT; the rate-limiting enzyme in *de novo* PC synthesis) and sulfatide synthase (SGalCerS) were determined by quantitative real-time PCR in KD and Ctr cells (Fig. 5). While no changes were observed for GlcCerS and SGalCerS, the level of GalCerS was over 8-fold higher in KD cells ($P = 0.001$). Expression of LacCerS and CCT were significantly reduced ($P < 0.0001$ and 0.03, respectively).

4. Discussion

We have demonstrated that ABCA2 deficiency delays the metastatic phenotype in the TRAMP prostate cancer model, up to 25 weeks of age, and inhibits chemotatic migration in a knockdown cell model. Even though primary tumors in KO/Tg and WT/Tg mice progress with similar histological grades and proliferative indices, no metastatic tumors were found in KO/Tg mice. These results suggest ABCA2-deficiency inhibits metastatic progression beyond the primary epithelial prostate tumors and/or alters metastatic favorability of the tumor microenvironment. We confirmed that ABCA2 KD in D6P2T cells inhibits chemotactic migration (a classic characteristic of metastatic cancer cells), but not random migration. These KD cells demonstrated altered expression of GalCerS and CCT,

implicating that changes in sphingolipid metabolism may contribute to the loss of chemotactic potential.

Since previous studies have only shown expression of ABCA2 in prostate cancer cell lines and normal prostate cDNA, we sought to examine baseline expression of the transporter in the TRAMP tumor model. ABCA2 expression in dorsal prostate was elevated in WT/Tg versus WT mice, thereby validating ABCA2 as a potential modulator of tumor progression in this model.

KO/Tg primary prostate lesions are similar to WT/Tg in terms of prostate volume, pathological progression and proliferative index. However, KO/Tg mice lack the metastatic tumors in lung and lymph nodes, as well as large, poorly differentiated tumors that present in WT/Tg littermates.

Surprisingly, SV tissue in 20 week-old KO/Tg mice was significantly enlarged compared to WT/Tg, as determined by MRI volumetry. The statistical significance of this disparity was lost by 25 weeks of age. Expression of vimentin, a marker of the epithelial-mesenchymal transition, was expressed at similar levels in the prostate, but was elevated in normal SV tissue in these 20 week-old KO/Tg mice. Others have reported that prostate tumors originating from the lateral lobe can cause obstruction and an increase in SV size and weight [24]. This may be exacerbated by increased vimentin expression, a protein that structurally increases the elasticity of endothelium [25] in the lamina propria. This could also create an environment conducive to the outgrowth of SV tumors and/or distention of the vesicles by seminal fluid. Further study is needed to determine the cause of this enlarged SV phenotype in KO/Tg mice.

Malignant tumors in the TRAMP model typically arise from carcinomas of the prostatic epithelium. However, one report described malignant tumors deriving from epithelial-stromal SV tumors [18]. Because of the absence of pathologically advanced tumors and a smaller average volume of WT/Tg SV, we presume that the metastatic tumors in WT/Tg are derived from the prostate rather than the SV. No changes in vimentin or desmin expression were observed among SV tumors of KO/Tg or WT/Tg mice, suggesting differentiation of SV tumors is unaffected by ABCA2 deficiency.

Although a precise role for ABCA2 in metastasis has yet to be determined, we have demonstrated a definitive delay in the events leading to metastasis of the lung and pelvic lymph nodes in KO/Tg mice. Global ABCA2 deficiency may impact a metastatic phenotype by causing a decrease in sphingomyelin (SM). Tissues of Abca2 null mice [7] have a significant decrease in SM levels compared to wild-type. Others have observed that prostate cancer cells rely on elevated SM levels to maintain a highly metastatic phenotype [13]. The reduced levels of SM in tissues from Abca2 null mice [6;7] may be causal to the inhibition or delay in metastatic progression. Our data show a significant elevation in GalCerS and a decrease in CCT expression [the rate-limiting enzyme in phosphatidylcholine (PC) synthesis] in ABCA2 KD cells. In an ABCA2-deficient environment, reduced levels of sphingomyelin (SM) may result from diminished PC pools available as a substrate for conversion of ceramide into SM (Fig. 5). Similarly, over-expression of the enzyme, GalCerS, may decrease the pool of sphingolipids available for SM synthesis. Application of exogenous galactosylceramide has shown anti-tumor and anti-metastatic effects via invocation of natural killer like T-cells (NKT), [26;27]. Further studies to determine whether similar mechanisms occur in KO/Tg mice are warranted.

Other ABC transporters have been linked with metastatic disease, namely ABCB1, ABCC1 and ABCC4 [28]. In addition, ABCA1, the closest homolog to ABCA2, is critical for sphingosine-1-phosphate (S1P) efflux from astrocytes [29]. S1P is a mediator of cell

invasion, motility and angiogenesis [30]. Pools of sphingosine, the precursor of S1P, are supplied by the degradation of SM [31].

Increased GM3 levels have also been associated with metastasis and tumor cell invasion in human and mouse urinary bladder tumors [32]. GT1b and GQ1b are downstream metabolites of tumor-associated gangliosides (GD3, GM2 and GD2) and have been shown to inhibit cell proliferation in melanoma cell lines [32]. Interestingly, GT1b and GQ1b are elevated in ABCA2 null mouse tissue [7]; however, the levels of the tumor-associated gangliosides (GM3, GM2, GD2) have not been analyzed.

Taken together, our results suggest that ABCA2 may have an important function for cancer cell chemotaxis and metastatic progression of prostate tumors. Future studies will help elucidate how ABCA2 deficiency alters the composition and/or localization of critical sphingolipids to impede the progression of metastatic disease.

Acknowledgments

This work and J.T. Mack were supported by the National Institutes of Health Ruth L. Kirschstein NRSA Fellowship CA117749. We thank Margaret Romano of the Department of Pathology & Laboratory Medicine for assistance with histological processing, sectioning and equipment for antigen retrieval, and Dr. Mehmet Bilgen and Peter Chou of the Preclinical Imaging in Translational Research Core for assistance with MR imaging of mice.

References

[1]. Mack JT, Brown CB, Tew KD. ABCA2 as a therapeutic target in cancer and nervous system disorders. Expert Opin Ther Targets. 2008; 12:491–504. [PubMed: 18348684]

[2]. Vulevic B, Chen Z, Boyd JT, Davis W Jr. Walsh ES, Belinsky MG, Tew KD. Cloning and characterization of human adenosine 5′-triphosphate-binding cassette, sub-family A, transporter 2 (ABCA2). Cancer Res. 2001; 61:3339–3347. [PubMed: 11309290]

[3]. Ile KE, Davis W Jr. Boyd JT, Soulika AM, Tew KD. Identification of a novel first exon of the human ABCA2 transporter gene encoding a unique N-terminus. Biochim Biophys Acta. 2004; 1678:22–32. [PubMed: 15093135]

[4]. Kaminski WE, Piehler A, Pullmann K, Porsch-Ozcurumez M, Duong C, Bared GM, Buchler C, Schmitz G. Complete coding sequence, promoter region, and genomic structure of the human ABCA2 gene and evidence for sterol-dependent regulation in macrophages. Biochem Biophys Res Commun. 2001; 281:249–258. [PubMed: 11178988]

[5]. Mack JT, Townsend DM, Beljanski V, Tew KD. The ABCA2 transporter: intracellular roles in trafficking and metabolism of LDL-derived cholesterol and sterol-related compounds. Curr Drug Metab. 2007; 8:47–57. [PubMed: 17266523]

[6]. Mack JT, Beljanski V, Soulika AM, Townsend DM, Brown CB, Davis W, Tew KD. “Skittish” Abca2 knockout mice display tremor, hyperactivity, and abnormal myelin ultrastructure in the central nervous system. Mol Cell Biol. 2007; 27:44–53. [PubMed: 17060448]

[7]. Sakai H, Tanaka Y, Tanaka M, Ban N, Yamada K, Matsumura Y, Watanabe D, Sasaki M, Kita T, Inagaki N. ABCA2 deficiency results in abnormal sphingolipid metabolism in mouse brain. J Biol Chem. 2007; 282:19692–19699. [PubMed: 17488728]

[8]. Laing NM, Belinsky MG, Kruh GD, Bell DW, Boyd JT, Barone L, Testa JR, Tew KD. Amplification of the ATP-binding cassette 2 transporter gene is functionally linked with enhanced efflux of estramustine in ovarian carcinoma cells. Cancer Res. 1998; 58:1332–1337. [PubMed: 9537224]

[9]. Punzi JS, Duax WL, Strong P, Griffin JF, Flocco MM, Zacharias DE, Carrell HL, Tew KD, Glusker JP. Molecular conformation of estramustine and two analogues. Mol Pharmacol. 1992; 41:569–576. [PubMed: 1545778]

[10]. Boonstra R, Timmer-Bosscha H, van Echten-Arends J, van der Kolk DM, van den Berg A, de Jong B, Tew KD, Poppema S, de Vries EG. Mitoxantrone resistance in a small cell lung cancer

cell line is associated with ABCA2 upregulation. Br J Cancer. 2004; 90:2411–2417. [PubMed: 15150577]

[11]. Ho MM, Ng AV, Lam S, Hung JY. Side population in human lung cancer cell lines and tumors is enriched with stem-like cancer cells. Cancer Res. 2007; 67:4827–4833. [PubMed: 17510412]

[12]. Hu Y, Wang M, Veverka K, Garcia FU, Stearns ME. The ABCA5 protein: a urine diagnostic marker for prostatic intraepithelial neoplasia. Clin Cancer Res. 2007; 13:929–938. [PubMed: 17289887]

[13]. Dahiya BBR, Goldberg BC, Yoon WH, Konety B, Chen K, Yen TS, Blumenfeld W, Narayan P. Metastasis-associated alterations in phospholipids and fatty acids of human prostatic adenocarcinoma cell lines. Biochem Cell Biol. 1992; 70:548–554. [PubMed: 1333235]

[14]. Hannun YA OL. Principles of bioactive lipid signalling: lessons from sphingolipids. Nat Rev Mol Cell Biol. 2008; 9:139–150. [PubMed: 18216770]

[15]. Greenberg NM, DeMayo F, Finegold MJ, Medina D, Tilley WD, Aspinall JO, Cunha GR, Donjacour AA, Matusik RJ, Rosen JM. Prostate cancer in a transgenic mouse. Proc Natl Acad Sci U S A. 1995; 92:3439–3443. [PubMed: 7724580]

[16]. Suttie A, Nyska A, Haseman JK, Moser GJ, Hackett TR, Goldsworthy TL. A grading scheme for the assessment of proliferative lesions of the mouse prostate in the TRAMP model. Toxicol Pathol. 2003; 31:31–38. [PubMed: 12597447]

[17]. Tani ASY, Flake GP, Nyska A, Maronpot RR. Epithelial-stromal tumor of the seminal vesicles in the transgenic adenocarcinoma mouse prostate model. Vet Pathol. 2005; 42:306–314. [PubMed: 15872376]

[18]. Yeh RLRIT, Kumar AP. Malignancy arising in seminal vesicles in the transgenic adenocarcinoma of mouse prostate (TRAMP) model. Prostate. 2009; 69:755–760. [PubMed: 19170049]

[19]. Bansal R, Pfeiffer SE. Regulated galactolipid synthesis and cell surface expression in Schwann cell line D6P2T. J Neurochem. 1987; 49:1902–1911. [PubMed: 2824698]

[20]. Tang SWJX, Wang X, Liu Z, Bahr SM, Sun SY, Brat D, Gutmann DH, Ye K. Akt phosphorylation regulates the tumour-suppressor merlin through ubiquitination and degradation. Nat Cell Biol. 2007; 9:1199–1207. [PubMed: 17891137]

[21]. Degrassi A, Russo M, Scanziani E, Giusti A, Ceruti R, Texido G, Pesenti E. Magnetic resonance imaging and histopathological characterization of prostate tumors in TRAMP mice as model for pre-clinical trials. Prostate. 2007; 67:396–404. [PubMed: 17187397]

[22]. Chen GWYMH, Tse GM, Moriya T, Lui PC, Zin ML, Bay BH, Tan PH. Expression of basal keratins and vimentin in breast cancers of young women correlates with adverse pathologic parameters. Mod Pathol. 2008; 21:1183–1191. [PubMed: 18536655]

[23]. Chen ZJ, Vulevic B, Ile KE, Soulika A, Davis W Jr. Reiner PB, Connop BP, Nathwani P, Trojanowski JQ, Tew KD. Association of ABCA2 expression with determinants of Alzheimer's disease. Faseb J. 2004; 18:1129–1131. [PubMed: 15155565]

[24]. Gingrich RJBJR, Foster BA, Greenberg NM. Pathologic progression of autochthonous prostate cancer in the TRAMP model. Prostate Cancer Prostatic Dis. 1999; 2:70–75. [PubMed: 12496841]

[25]. Storm JJPC, MacKintosh FC, Lubensky TC, Janmey PA. Nonlinear elasticity in biological gels. Nature. 2005; 435:191–194. [PubMed: 15889088]

[26]. Nishihori KKY, Tanaka M, Okamoto T, Hagiwara S, Araki N, Kogawa K, Kuribayashi K, Nakamura K, Niitsu Y. Interleukin-2 gene transfer potentiates the alpha-galactosylceramide-stimulated antitumor effect by the induction of TRAIL in NKT and NK cells in mouse models of subcutaneous and metastatic carcinoma. Cancer Biol Ther. 2009; 8:1763–1770. [PubMed: 19901518]

[27]. Smyth NYCMJ, Pellicci DG, Kyparissoudis K, Kelly JM, Takeda K, Yagita H, Godfrey DI. Sequential production of interferon-gamma by NK1.1(+) T cells and natural killer cells is essential for the antimetastatic effect of alpha-galactosylceramide. Blood. 2002; 99:1259–1266. [PubMed: 11830474]

[28]. Fletcher MHJI, Henderson MJ, Norris MD. ABC transporters in cancer: more than just drug efflux pumps. Nat Rev Cancer. 2010; 10:147–156. [PubMed: 20075923]

[29]. Sato EMK, Horiuchi Y, Mogi C, Tomura H, Tosaka M, Yoshimoto Y, Kuwabara A, Okajima F. Critical role of ABCA1 transporter in sphingosine 1-phosphate release from astrocytes. J Neurochem. 2007; 103:2610–2619. [PubMed: 17931360]

[30]. Kim KTRH, Milstien S, Spiegel S. Export and functions of sphingosine-1-phosphate. Biochim Biophys Acta. 2009; 1791:692–696. [PubMed: 19268560]

[31]. Tani TSM, Ito M, Igarashi Y. Mechanisms of sphingosine and sphingosine 1-phosphate generation in human platelets. J Lipid Res. 2005; 46:2458–2467. [PubMed: 16061940]

[32]. Dyatlovitskaya AGKEV. Role of biologically active sphingolipids in tumor growth. Biochemistry (Moscow). 2006; 71:10–17. [PubMed: 16457613]

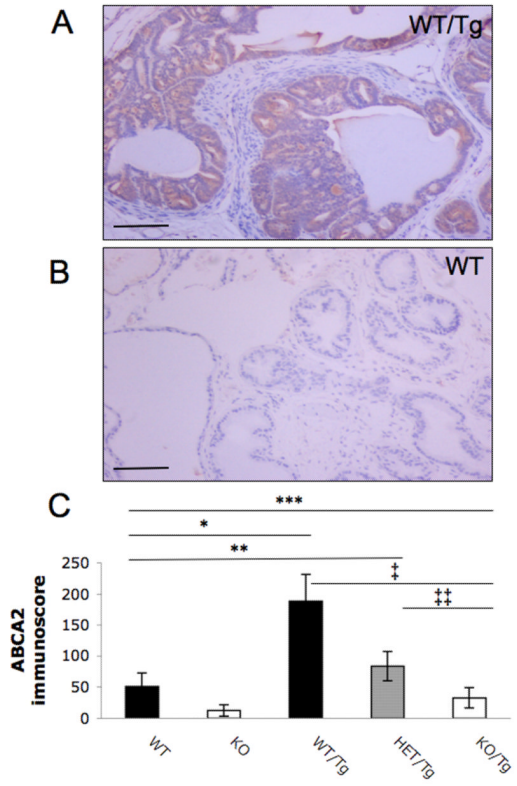

Fig. 1.

ABCA2 expression is elevated in TRAMP prostatic epithelia compared to WT. Immunohistochemical analysis of dorsal prostate at 20 weeks of age reveals a significant elevation in ABCA2 expression in TRAMP prostate (A) compared to that of WT (B). (C) Average immunoscore for relative ABCA2 expression in WT dorsal prostate is significantly lower than WT/Tg (**P* <0.0001), HET/Tg (***P* = 0.008), but not of KO/Tg (*P* = 0.16). Immunoscores of KO/Tg prostate are significantly lower than WT (****P* < 0.01), WT/Tg (‡*P* < 0.0001) and HET/Tg (‡‡ *P* = 0.002). The KO and KO/Tg samples correct for background staining of the anti-ABCA2 rabbit polyclonal antibody. Images were taken at 10× magnification. Scale bar represents 100 μm.

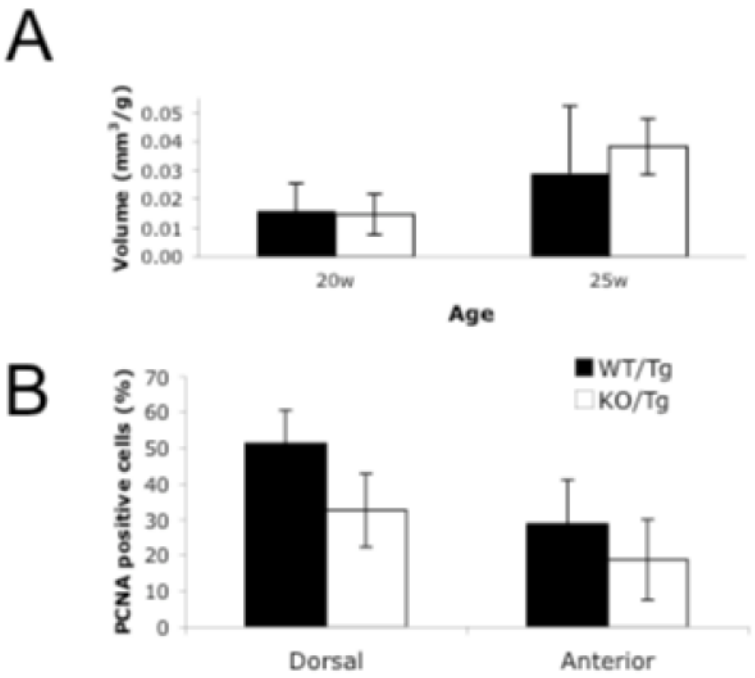

Fig. 2.

ABCA2 deficiency does not impact prostate volume or proliferation of epithelial lesions in primary prostate tumors. (A) Average prostate volume as determined using MRI volumetry did not differ at 20 or 25 weeks of age between WT/Tg and KO/Tg mice (indicated with closed and open bars, respectively; mean +/− standard deviation). (B) Proliferating cell nuclear antigen (PCNA) immunostaining demonstrated similar proliferative indices among epithelial cells of both dorsal and anterior prostatic lesions ($P > 0.2$; N= 5 mice per group, mean +/− standard error).

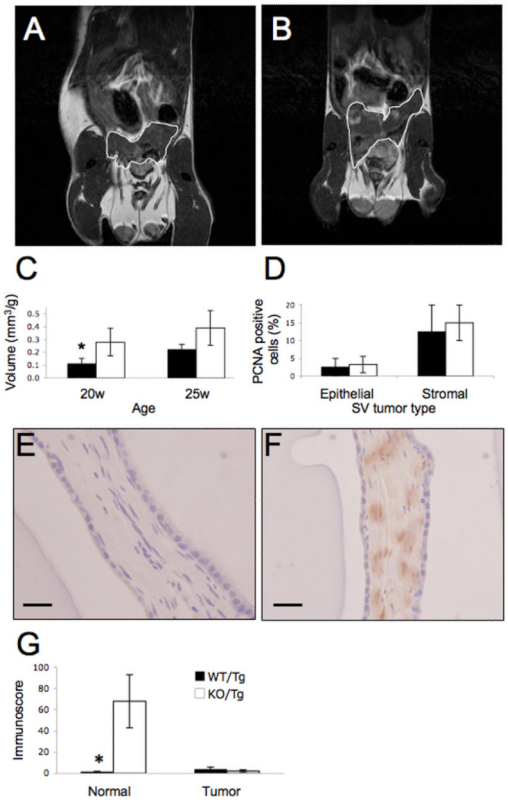

Fig. 3.

Seminal vesicle (SV) volume and vimentin expression are greater in KO/Tg mice at 20 weeks, but proliferative capacity of SV tumors is similar to WT/Tg. Representative MR images (SV tissue outlined in white) of WT/Tg (A) and KO/Tg (B) littermates at 20 weeks of age. (C) SV volume, as determined by MRI volumetry, is significantly greater in 20 week-old KO/Tg mice (*P < 0.01), with that of 25 week-old mice falling short of significance ($P > 0.1$). (D) Proliferative index, determined by PCNA immunohistochemistry, is unaffected by ABCA2 deficiency in both epithelial and stromal lesions of the seminal vesicle ($P > 0.7$). Vimentin immunohistochemistry in normal SV tissue of WT/Tg (E) and KO/Tg (F) reveals a marked increase in vimentin positive stromal cells within the lamina propria of KO/Tg mice (G; *$P = 0.02$); however, vimentin expression is equivalently low in SV tumors of KO/Tg and WT/Tg animals (G). Scale bars are equivalent to 20 μm. N= 5 mice per group, mean ± standard deviation shown; WT/Tg and KO/Tg indicated by closed and open bars, respectively.

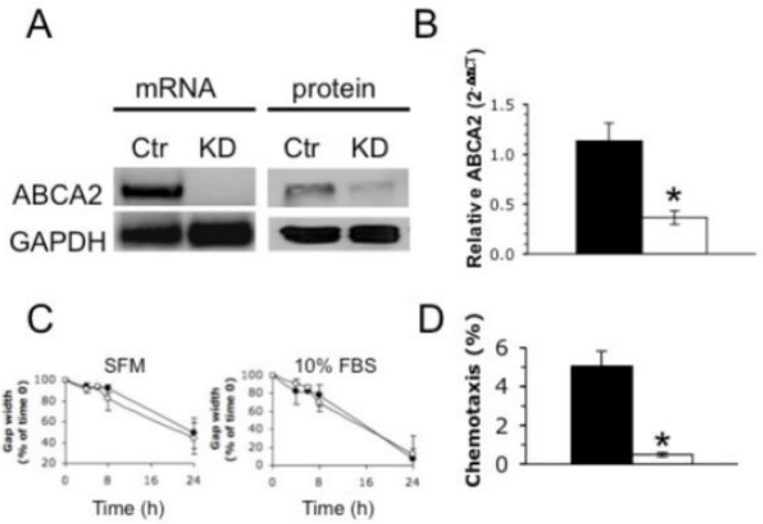

Fig. 4.

Stable shRNA-based knockdown of ABCA2 in D6P2T cells results in decreased chemotactic migration. Compared to shRNA control (Ctr) a significant (75-80%) knockdown (KD) was achieved in ABCA2 mRNA and protein, as determined by RT-PCR and Western blot densitometry (A); mRNA KD was confirmed by quantitative real-time PCR (B; **P* = 0.0006). The rate of random migration was indistinguishable between Ctr (closed circles) and KD cells (open circles) in a would-healing assay in the presence of either serum-free (SFM) or 10% FBS-containing media (C). However, KD cells exhibited a significant decrease in the percentage of cells undergoing chemotaxis from SFM to 10% FBS-containing media in an 8 μm transwell chamber (D; **P* = 0.0004; mean ± standard deviation).

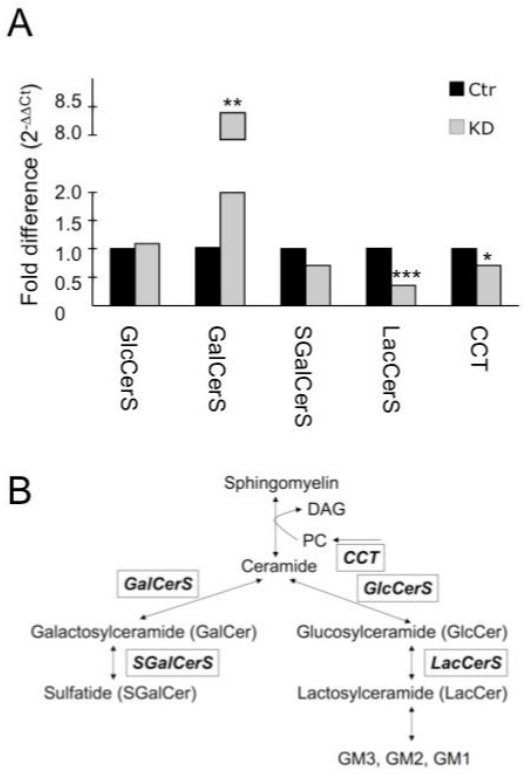

Fig. 5.

ABCA2 deficiency impacts expression of glycosphingolipid biosynthetic enzymes. (A) Levels of GalCerS are over 8-fold higher in ABCA2 knockdown (KD) cells compared to D6P2T control (Ctr) cells as confirmed by quantitative real-time PCR (***P* = 0.001). Expression of LacCerS and CCT are significantly reduced (****P* < 0.0001 and *P = 0.03, respectively). (B) Schematic for enzymes involved in sphingolipid metabolism. Abbreviations: GalCerS (galactosylceramide synthase) GlcCerS (glucosylceramide synthase), SGalCerS (sulfatide synthase), LacCerS (lactosylceramide synthase), CCT (CTP: choline cytidylyltransferase).

Table 1

Primers sequences for quantitative real-time PCR

Gene	Primer pair (Forward, Reverse)
ABCA2	GTCGACCTCATCAAGACAGGACGTTCAGTGG, CTCGAGTCAGCAGAGCGTATCGGTGTTGAAG
GAPDH	GGATCCACCACAGTCCATGCCATCAC, AAGCTTTCCACCACCCTGTTGCTGTA
GlcCerS	AGTGTGTGACGGGGATGTCT, CTTCCGCAATGTACTGAGCA
GalCerS	ACGAGAGAGGCCATCACACT, GGTATCGCTGGAGGCTGTAG
SGalCerS	ACTACTTTGGGTCCGTGGTG, CGAAGAAGAGCAGGTTACGG
LacCerS	CATGAACACCTCCCGATCTT, TTCATGGCCTCTTTGAAACC
CCT	GCCAGCTCCTTTTTCTGATG, CCTGCAGGCTTCTTCCATAG

Table 2

Primary prostate tumor pathology and occurrence of metastatic tumors

		Primary Prostate Tumors			Metastatic Tumors	
Genotype	**age (w)**	**Pathological Score***	**Mean ± SD**	**PD‡**	**Lung**	**Lymph node**
WT/Tg	20	8			X	X
		10				
		12			**	
		8				
		8	9± 2			
	25	10			**	
		18		X	X	X
		11	13 ± 4			X
KO/Tg	20	8				
		10				
		9				
		8	9 ± 1			
	25	11				
		11				
		11	11 ± 0			

X Metastatic tumor in this tissue

*Pathological score based on the methods by Suttie *et al*. 2003 [16]

‡Poorly differentiated tumor

**Hyperproliferation in this tissue

Table 3

Incidence of large (>7g) poorly differentiated tumor masses in mice (20-30w)

Genotype	PD Prostate Tumor	Other (Mammary)	Total
WT/Tg	2/9	1/9	3/9
KO/Tg	0/8	0/8	0/8